

Research Article

Effects of MAPP Compatibilization and Acetylation Treatment Followed by Hydrothermal Aging on Polypropylene Alfa Fiber Composites

Noura Hamour,¹ Amar Boukerrou,¹ Hocine Djidjelli,¹
Jean-Eudes Maigret,^{2,3,4} and Johnny Beaugrand^{2,3}

¹Laboratoire des Matériaux Polymères Avancés (LMPA), Faculté de Technologie, Université Abderrahmane Mira, 06000 Bejaia, Algeria

²INRA, UMR614 Fractionnement des AgroRessources et Environnement, 51100 Reims, France

³Université de Reims Champagne-Ardenne, UMR614 Fractionnement des AgroRessources et Environnement, 51100 Reims, France

⁴INRA, UR1268 Biopolymères Interactions Assemblages, rue de la Geraudiere, 44316 Nantes, France

Correspondence should be addressed to Noura Hamour; nherroudj@yahoo.fr

Received 8 January 2015; Revised 28 March 2015; Accepted 29 March 2015

Academic Editor: Saiful Islam

Copyright © 2015 Noura Hamour et al. This is an open access article distributed under the Creative Commons Attribution License, which permits unrestricted use, distribution, and reproduction in any medium, provided the original work is properly cited.

This work investigates the effect of hydrothermal aging on the properties of polypropylene/alfa fiber composites. Hydrothermal aging was induced in an environmental testing chamber at 65°C and 75% relative humidity (RH) over a 1000 h period. At the beginning ($t = 0$ h), the results showed that Young's moduli of the untreated alfa fibers and the acetylation-treated fibers increased by 21% and 36%, respectively, compared with the virgin polypropylene (PP). Additionally, Young's moduli decreased by 7% for the compatibilized composites composed of maleic anhydride grafted polypropylene (MAPP). After 1000 h of aging, Young's moduli decreased by 36% for untreated alfa fibers and 29% for the acetylation-treated alfa fibers and the compatibilized composites. Significant degradation was observed in the untreated alfa fiber samples. The Fourier transformed infrared (FTIR) allows us to distinguish the characteristic absorption bands of the main chemical functions present in the composite material before and after aging. The thermal properties showed that the thermal stability and the degree of crystallinity of the composites decreased after hydrothermal aging; this result was corroborated by the dynamical mechanical analysis (DMA) results.

1. Introduction

In recent years, substantial attention has been focused on the development of environmentally friendly composites that combine synthetic polymers with plant-based fibers. Natural fibers such as alfa [1, 2] olive husk [3], wood [4, 5], luffa [6], coir [7], hemp [8], kenaf [9], and sisal [10] have been widely used in composites. They are used as reinforcement for the polymer matrix and have good potential to replace conventional fibers (glass, carbon, etc.) in certain applications [11]. Moreover, lignocellulosic fibers are a biodegradable material obtained from renewable and abundant sources with low extraction prices [12]. However, the hydrophilic nature of natural fibers can be a disadvantage for composite manufacturing because these fibers lack compatibility with

hydrophobic polymeric matrices, which may result in poor performance. To solve this problem, chemical modification of natural fibers or the use of compatibilizer agents has been necessary. However, composites based on natural fibers present poor dimensional stability when in contact with water [13]. The possibility of using these materials in outdoor applications necessitates analyses of their mechanical behavior under the influence of hydrothermal aging [14]. Lignocellulose fibers (or plant fibers) contain many hydroxyl groups and readily interact with water molecules via hydrogen bonding. In contrast to glass fibers, in which water adsorption occurs at the surface, lignocellulosic fibers can interact with water throughout their bulk. The quantity of sorbed water depends on the relative humidity of the surrounding atmosphere and the degree of crystallinity. All of the hydroxyl groups in the

TABLE I: Overview of the samples tested.

Designations		Analysis					
Abbreviations	Compositions	FTIR	Tensile test	ATG/DSC	DMTA	SEM	
		Aging Kinetic Analysis (h)					
Virgin PP	100% PP	0; 1000	0; 150; 400; 600; 800; 1000	0; 1000	0; 1000	0; 1000	
F20UT	Fiber 20 wt% + 80% PP	0; 1000	0; 150; 400; 600; 800; 1000	0; 1000	0; 1000	0; 1000	
F20AT	Acetylated fiber 20 wt% + 80% PP	0; 1000	0; 150; 400; 600; 800; 1000	0; 1000	0; 1000	0; 1000	
F20AMAT	Fiber 20 wt% + 5 wt% Compatibiliser + 75% PP	0; 1000	0; 150; 400; 600; 800; 1000	0; 1000	0; 1000	0; 1000	

amorphous phase are assumed accessible by polar solutions, which is unlike crystalline phases, in which only the surfaces are available for water sorption. Therefore, swelling by water uptake can lead to microcracking of composites and the degradation of mechanical properties [13, 15].

This study aims to improve the understanding of the effect of hydrothermal aging of PP/alfa fiber composites. In addition, this study investigates the modification of interfacial adhesion forces between the alfa fibers (high hydrophilicity) and the PP matrix (strongly hydrophobic) to increase their compatibility using two different methods. The first method was based on the chemical treatment of alfa fibers through acetylation by reacting the hydroxyl groups of the lignocellulosic material with the acetyl groups of acetic anhydride (Ac). The second method consisted of using the well-known polymer maleic anhydride grafted polypropylene (MAPP) as a compatibilizer to improve the interfacial bonding between the alfa fibers and the PP matrix. These two composites were compared to a PP/untreated alfa fiber composite. The three composite materials obtained were studied using several analytical techniques, including FTIR spectroscopy, the measurement of tensile and dynamic mechanical properties (DMA) and thermal stability (TGA, DSC), and SEM observations.

2. Materials and Methods

2.1. Materials. Alfa plants were collected in western Algeria. After in-house decortication, the fraction of the material obtained after sieving through a 100 μm mesh was used. The chemical composition of the alfa grass was mainly lignin (29 wt%), cellulose (45 wt%), and hemicelluloses (20 wt%). These constituents were determined using previously described chemical procedures [16]. The isotactic polypropylene (PP500P $\text{\textcircled{c}}$) used in this study as the matrix was provided by SABIC (Saudi Arabia) with a melt flow index (MFI) of 3 g/10 min (230 $^{\circ}\text{C}$ /2.16 kg) (ASTM D-1238) and a density of 0.9 g $\cdot\text{cm}^{-3}$ (values from supplier datasheets). Maleic anhydride (MAPP), supplied by ARKEMA (France), has a melt flow index (MFI) of 2.63 g/10 min (190 $^{\circ}\text{C}$ /235 g, technical notice). Acetic anhydride (Ac, 98%), acetic acid, and sulfuric acid were provided by Sigma-Aldrich.

2.2. Acetylated Alfa Fibers. Dry alfa fiber (15 g) was placed in a round-bottom flask with 72.5 mL acetic acid. The reaction was performed in a thermostatic bath at 35 $^{\circ}\text{C}$ for 45 min under mechanical stirring. Then, 24 mL of acetic acid was

added along with 0.1 mL of concentrated H_2SO_4 and the bath was maintained for 1 h. After this step, the mixture was cooled to 18 $^{\circ}\text{C}$ for the slow addition of acetic anhydride (40 mL) with 0.6 mL concentrated H_2SO_4 over 3 h with constant stirring. A temperature of 24 $^{\circ}\text{C}$ was maintained for more than 15 min. Then, the temperature was slowly increased to 50–55 $^{\circ}\text{C}$ and the reaction continued for 3 h. This mixture was vacuum filtered, washed with distilled water, and then dried in an oven at 50 $^{\circ}\text{C}$ for 24 h [17].

2.3. Composite Processing. Different formulations of PP/alfa fibers were prepared using “corotating” twin-screw extrusion. In addition to neat PP, PP/untreated alfa fiber composites, PP/alfa fiber composites treated with acetic anhydride, and a compatibilized composite were prepared after twin-screw extrusion. The formulations were injected using an injection press (ERINKA mark) connected to the compounder. Tensile specimens (ISO 527-5B) were obtained as the output of the injection-molding machine. The mould temperature were kept at 180 and 30 $^{\circ}\text{C}$, respectively at different pressures (4 bar for preinjection and 5 bar for injection). Table 1 shows an overview of the samples tested.

2.4. Hydrothermal Aging Treatment. The alfa fiber/polypropylene composites were placed in a Secasi Technologies (SLH41/08P, France) environmental testing chamber equipped with a relative humidity controller with a precision of $\pm 2\%$ to $\pm 5\%$. Demineralized water was used throughout the duration of treatment to ensure the neutrality of the environment. A relative humidity (RH) of 75% and temperature of 65 $^{\circ}\text{C}$ were used to conduct the aging treatments. The samples were aged for different periods: 150, 400, 600, 800, and 1000 h (approximately 6 to 41 days).

2.5. Fourier Transform Infrared Spectroscopy (FTIR). FTIR spectra of the PP and PP/alfa fiber composites with and without aging were recorded using an FTIR SHIMADZU FTIR-8400S in the range of 4000–500 cm^{-1} . The equipment was operating in absorbance mode with 4 scan, at a resolution of 4 cm^{-1} , meaning a displacement of the mirror of 0.25 cm. Thin films, which were between 60 and 80 μm in thickness, were prepared by compression molding at 180 $^{\circ}\text{C}$ for 2 min.

2.6. Thermogravimetric Analysis (TGA). Thermogravimetric analysis (TGA) was performed using a Hi-Res TG 2950 (TA instruments) in an inert atmosphere at a heating rate of 10 $^{\circ}\text{C}/\text{min}$. The sample weights were in the range of 10–20 mg,

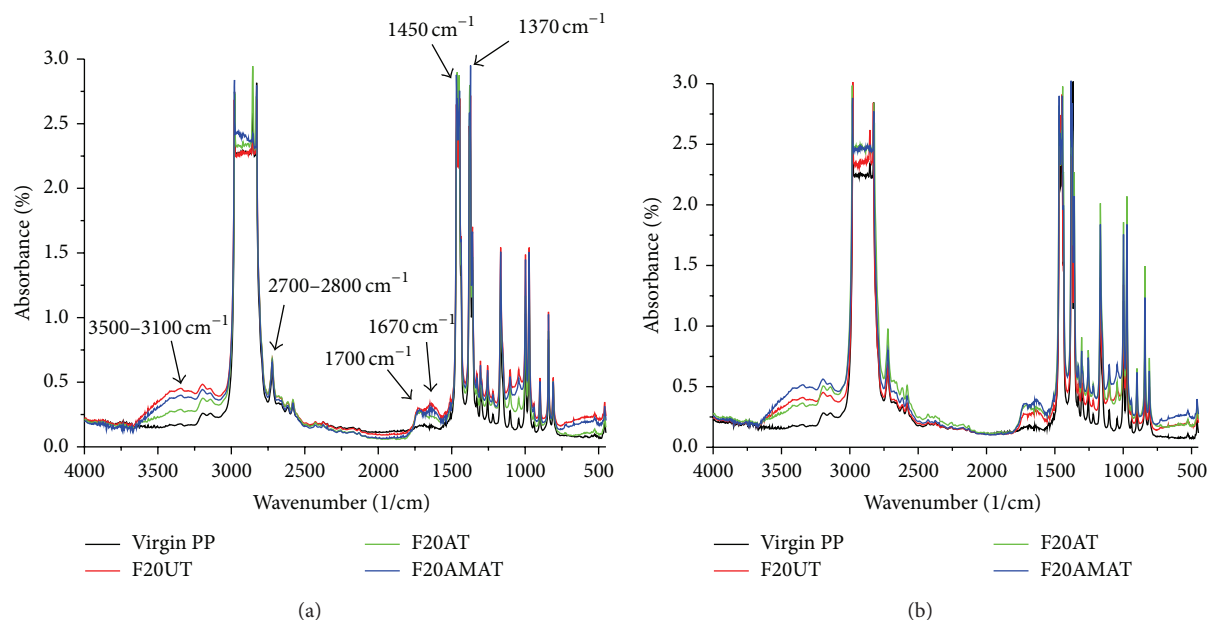


FIGURE 1: FTIR spectra of the PP/alfa fiber composites: (a) before aging and (b) after aging.

and they were scanned in the temperature range of 20°C to 700°C.

2.7. Differential Scanning Calorimetric Analysis (DSC). The DSC measurements were conducted using a DSC-2920 (TA instrument) differential scanning calorimeter with nitrogen as the purge gas. Samples of approximately 5–10 mg were analyzed in the temperature range of -50 to $+200^\circ\text{C}$. To erase the thermal history, the first cooling and the second heating thermograms were recorded with the following scanning rate: $10^\circ\text{C}/\text{min}$ in the first cooling and $10^\circ\text{C}/\text{min}$ in the second heating. The melting peak (T_m) was obtained. The melting temperature (T_f), melting enthalpy (ΔH_f), crystalline index (X_c), crystallization temperature (T_c), and crystallization enthalpy (ΔH_c) were determined from the DSC thermograms, and the values are reported in Table 3.

2.8. Tensile Tests. Quasi-static tensile tests were carried out using a Macro Test Well 108-2kN testing apparatus in a climatic room where the temperature was 23°C at 65% RH according to ISO 527-5B. The speed was 50 mm/min. The tests were performed at least three times for each sample, and the results were averaged arithmetically.

2.9. Dynamic Mechanical Analysis (DMA). Dry and moisture-saturated samples were subjected to dynamic mechanical analysis (DMA) using a tension cantilever system DMA Q800 (TA Instruments) at a frequency of 1 Hz and a driving force of 8 N. The dynamic storage moduli of each specimen were determined as a function of humidity from 10% to 100% (isotherm of 40°C).

2.10. Scanning Electron Microscopy (SEM). Scanning electron microscopy (SEM) was used to monitor the fracture surface

of the composites after the samples were frozen in liquid nitrogen. SEM analysis was performed using a TM 1000 Tabletop Microscope (Hitachi).

3. Results and Discussion

3.1. FTIR Analysis. To analyze the behavior of PP containing fibers as a function of the treatment and the applied hydrothermal aging, as well as the influence of aging on the mechanical and thermal behavior, spectroscopic techniques were employed to study the formation of radical and chemical species that affect the structure and final behavior of the composite. The technique employed was infrared (FTIR) spectroscopy. The results obtained and the FTIR spectra for the PP/untreated alfa fiber composites are shown in Figure 1(a). The results presented in Figure 1(a) show the presence of aldehyde carbonyl groups ($\text{C}=\text{O}$) at the stretch frequency of approximately 1700 cm^{-1} , C–H absorption within the range of $2700\text{--}2800\text{ cm}^{-1}$, and asymmetric stretching of the cis and trans $\text{C}=\text{C}$ at approximately 1670 cm^{-1} . Absorption bands typical of PP were also observed at frequencies between 1450 cm^{-1} for the $-\text{CH}_2$ bond and 1370 cm^{-1} for the $-\text{CH}_3$ bond. We also noticed the appearance of the absorption band between 3500 and 3100 cm^{-1} , which increases in intensity after aging Figure 1(b), reflecting elongation of the hydroxyl vibration of water molecules (OH) associated with the diffusion of the liquid within the matrix and fiber interface/matrix [18, 19].

In addition, the FTIR spectra results for the F20AT (PP/treated alfa fiber by acetylation) and F20AMAT (PP/alfa fiber/MAPP) composites are shown in Figures 1(a) and 1(b). As in the case of the virgin matrix and the untreated composite the spectra of F20AT F20AMAT composite present the same absorption bands. This result suggests that the presence

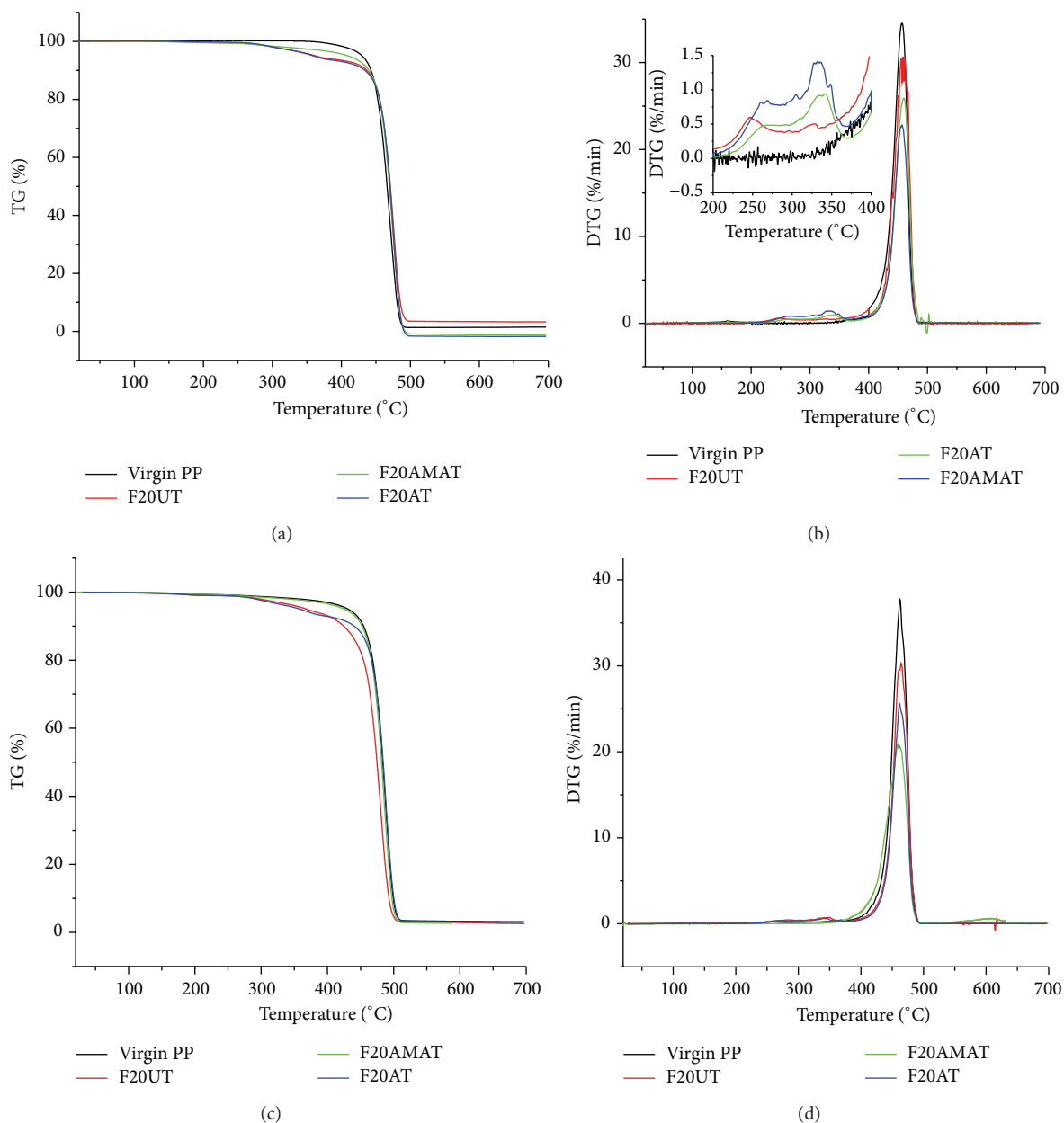


FIGURE 2: Thermal degradation behavior of the composites: ((a), (b)) before aging and ((c), (d)) after aging.

of a compatibilizing agent and the chemical modification by acetylation of fibers have no effect on the composite during the hydrothermal aging.

3.2. Thermogravimetric Analysis (TGA). Thermogravimetric analysis was used to determine the degradation temperature of the composites, as well as their components, under nitrogen atmosphere. Figure 2 clearly shows that the thermal degradation profiles of the composites with and without aging are similar. One stage of polypropylene degradation was recorded, which is unlike composites, whose degradation occurs in two steps [20]. Indeed, the PP decomposes from 400°C and gives mainly propylene trimer [21]. Beyond

500°C, oligomers of other monomers are also formed, and approximately 0.8% of char is recovered at the end of its decomposition. However, the thermal degradation of the alfa fiber-filled PP composites occur in a two-step process, this result was confirmed in derivative thermogravimetric curve (DTG) (Figure 2(b)). The first thermal degradation step may correspond to lignin and polysaccharide polymers (hemicellulose and cellulose). The second step was attributed to degradation of the polymer (PP) [22].

The incorporation of the untreated alfa fiber in polypropylene led to a decrease in the onset decomposition temperature; this decrease is probably caused by the decomposition of the components of the alfa fiber (cellulose,

TABLE 2: TGA data for neat PP and PP/alfa fiber composite materials.

Formulations		T_{onset} (°C)	V_{max} (%/min)	Char (Wt. %)
Before aging	Virgin PP	431	34.6	0.34
	F20UT	362	30.0	2.50
	F20AT	394	25.4	3.19
	F20AMAT	360	21.8	3.63
After aging	Virgin PP	393	35.0	0.23
	F20UT	353	29.8	3.26
	F20AT	395	24.1	3.54
	F20AMAT	307	20.5	3.42

TABLE 3: Crystallinity rates of neat PP and PP/alfa fiber composite materials.

Formulations		T_f (°C)	ΔH_f (J/g)	T_c (°C)	ΔH_c (J/g)	X_c (%)
Before aging	Virgin PP	116	94.2	169	77.0	36.8
	F20UT	115	87.0	170	74.4	44.5
	F20AT	116	83.4	170	74.5	44.5
	F20AMAT	115	80.1	170	72.4	43.3
After aging	Virgin PP	116	85.1	170	72.0	34.4
	F20UT	116	81.8	169	68.9	41.2
	F20AT	116	81.4	170	67.2	40.2
	F20AMAT	117	78.2	169	69.1	41.3

hemicellulose, and lignin). However, the thermal stability slightly improved for the PP/alfa fiber composites with the compatibilizing agent MAPP compared with the composites modified by acetylation and untreated composites, which is explained by the improved compatibility and adhesion of the fibers to the PP matrix [3].

The typical degradation temperatures of virgin PP and the PP/alfa fiber composites are summarized in Table 2. Moisture plays an important role in influencing the mechanical behavior, as well as the long-term durability, of the composites. Figures 2(c) and 2(d) show the thermograms for virgin PP and PP/alfa composites after aging. The derivatives of the mass loss curves are also displayed to highlight the differences between the samples.

The maximum degradation rate (V_{max}) decreased after aging. For the untreated composite (F20UT), the V_{max} decreased from 30 to 29 (%/min). Clearly, this decrease was due to the lignin, which acts as a heat stabilizer in the PP. However, the treated composite showed the same tendencies. The V_{max} decreased from 25 to 24 (%/min) and from 21 to 20 (%/min) for F20AT and F20AMAT, respectively. This decrease is due to the increase of the thermal stability.

3.3. Differential Scanning Calorimetry (DSC) Analysis. The percent crystallinity was obtained from DSC analysis using the following relation [23, 24]: $X_c (\%) = ((\Delta H)/(\Delta H_m \cdot \omega)) * 100$, where ΔH and ΔH_m are the heat of fusion of PP and 100% crystalline PP, respectively. A value of $\Delta H_m = 209$ J/g for PP [25] was used, and ω is the reinforcement content. The crystallinity of virgin PP and the PP/alfa fiber composites decreased after aging; the crystallinity of virgin PP decreased by 6% after aging, and the crystallinity of the

F20UT composite (PP/untreated alfa fiber) decreased by 7% after aging. Crystallinity reductions for the F20UT, F20AT, and F20AMAT composites were observed after hydrothermal aging (Table 3). Beg and Pickering [23] found similar results and explained that this reduction is related to the decrease of the molar mass of macromolecular chains. The other authors [26] have explained the crystallinity reduction by the decrease of the structural irregularity.

3.4. Effects of Hydrothermal Aging on the Mechanical Properties. Mechanical tests were performed on all of the samples before and after aging; the results are shown in Figures 3(a) and 3(b). In general, the mechanical properties of these materials decreased after moisture uptake due to the effect of the water molecules, which change the structure and properties of the fibers and the matrix as well as the interface between them [27]. After the water molecule penetrates the composite materials, the fibers tend to swell. The matrix structure can also be affected by the water uptake by processes such as chain reorientation and shrinkage. Additionally, water molecules are inserted between the macromolecular chains of polypropylene weakening secondary link of Van der Waals and therefore they reduce the interactions between these chains that can move freely. For this reason we can say that the water acts as a plasticizer. Hydrothermal aging causes the degradation of fibers in a thermoplastic matrix. Water absorption and its effects contribute to the loss of compatibilization between the fibers and the matrix, which results in debonding and weakening of the interface adhesion [27].

According to the obtained tensile strength results (Figure 3(a)), the values at the beginning ($t = 0$ h) are slightly

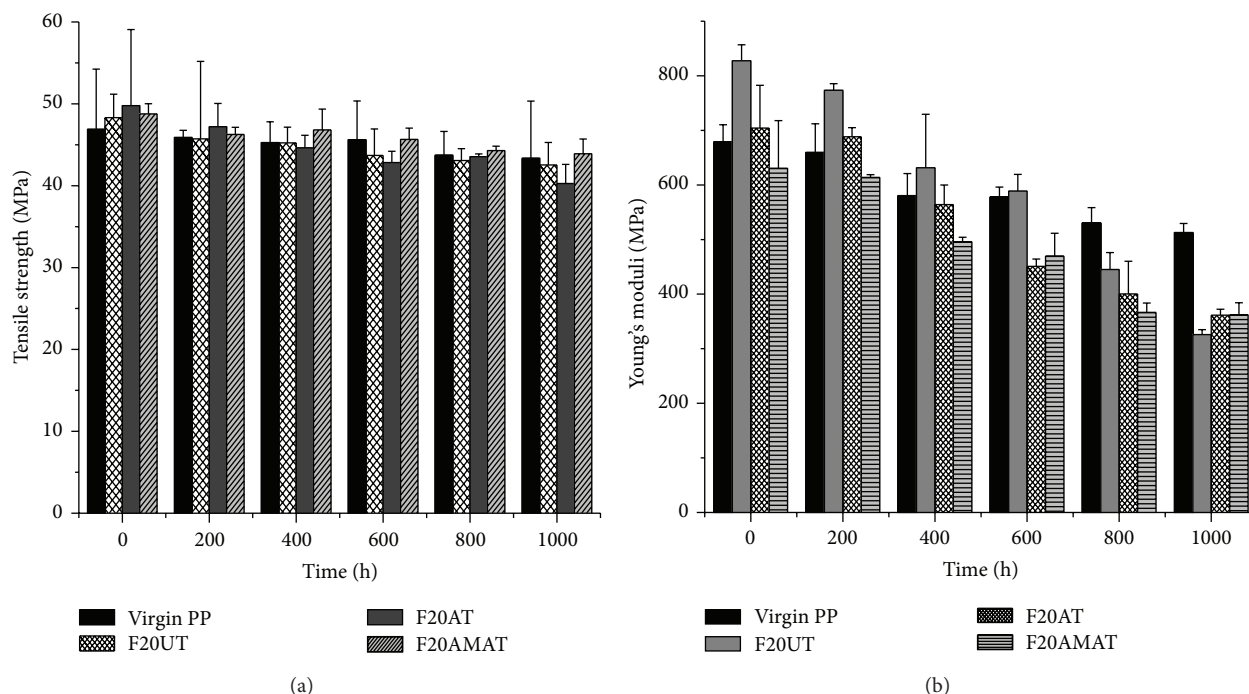


FIGURE 3: Evolution of the mechanical properties of the PP/alfa fiber composites: (a) tensile strength and (b) Young's moduli.

increased compared with those of the PP matrix after 1000 h. A slight decrease was observed for all of the composite mixtures.

At the beginning ($t = 0$ h), Young's moduli of the F20UT and F20AT composites were higher than that of the PP matrix, which was due to the fiber stiffness, in both of the different composites. However, the F20AMAT composite had the lowest Young modulus, which can be explained by the plasticization due to the MAPP compatibilizer. After 1000 h, the modulus decreased with exposure time to temperature and moisture, which acts as a plasticizer. Similar degradation behavior was observed by Hammiche et al. and Chen et al. [28, 29]. Finally, the changes in the mechanical properties coincided with the structural modification and chemical changes deduced from the FTIR characterization.

3.5. Dynamic Mechanical Analysis (DMA). Dynamic mechanical analysis is a method for measuring the viscoelasticity of polymers. This method enables the study and characterization of the mechanical properties as the storage moduli, E' , which represents the stiffness and the elastic component of the material. E' expresses the material's ability to store mechanical energy and to fully transfer the energy in the form of elastic deformation. The dynamic mechanical properties of virgin PP and the PP/alfa fiber composites with and without modification were evaluated. The storage moduli, E' , as a function of humidity is depicted in Figure 4(a). In the case of the matrix, the storage moduli, E' , significantly decreased with moisture due to gradual softening of the material and increased segmental mobility. Regardless of the humidity, after the addition of fibers (F20UT), a significant increase in the storage modulus was

observed, as expected. This result revealed that there is an effective stress transfer across the interface, which improves the stiffness of the composite. For the systems based on the compatibilized composites (F20AMAT), the storage moduli were slightly lower compared with those of the materials based on nonmodified fibers. This reduction can also be explained by a reduction of the stiffness. This result confirms the data obtained from the tensile measurements, which show a decrease in tensile modulus at room temperature for the compatibilized composites.

With increasing humidity, the E' values of the matrix PP and the composite systems decreased. However, for composites, the decreased matrix moduli are arguably compensated for by the fiber stiffness. The effects of hydrothermal aging on the dynamic mechanical behavior after aging are shown in Figure 4(b). The storage moduli of the composites containing fibers (treated or not) were slightly lower than that of the PP matrix. This decrease reflects several concurrent phenomena, which are reversible. The reversible phenomena are summarized by the plasticization caused by the presence of water. The hydrophilic nature [30] of natural fibers is considered to decrease the resistance of the composite in a humid environment. From these results, it can be deduced that a study of the behavior of the composites in a humid atmosphere is necessary not only to estimate the effects of aging but also to better understand the mechanisms involved to minimize them. Presumably, the first water molecules entering the polymer will act strongly on the matrix. These water molecules can initially spread in space (free volume and porosity) before reaching the polar sites, after which they generate swelling and, as a consequence, a change in thermomechanical properties. The mechanism of plasticization,

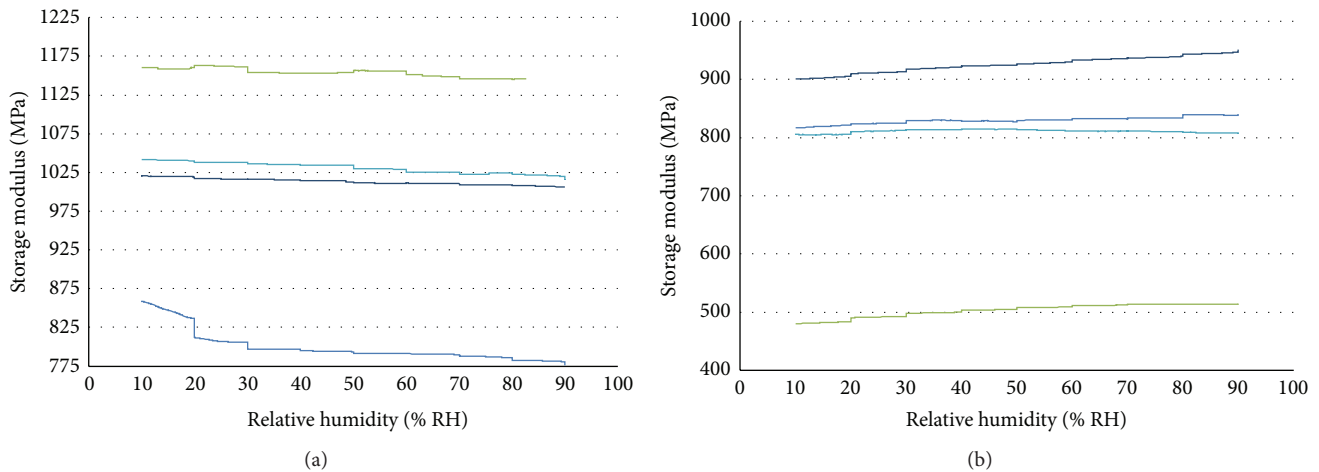


FIGURE 4: Variation of storage moduli versus humidity (DMTA analyses): (a) before aging and (b) after aging for (blue line) virgin PP, (green line) F20UT, (light blue line) F20AT, and (black line) F20AMAT.

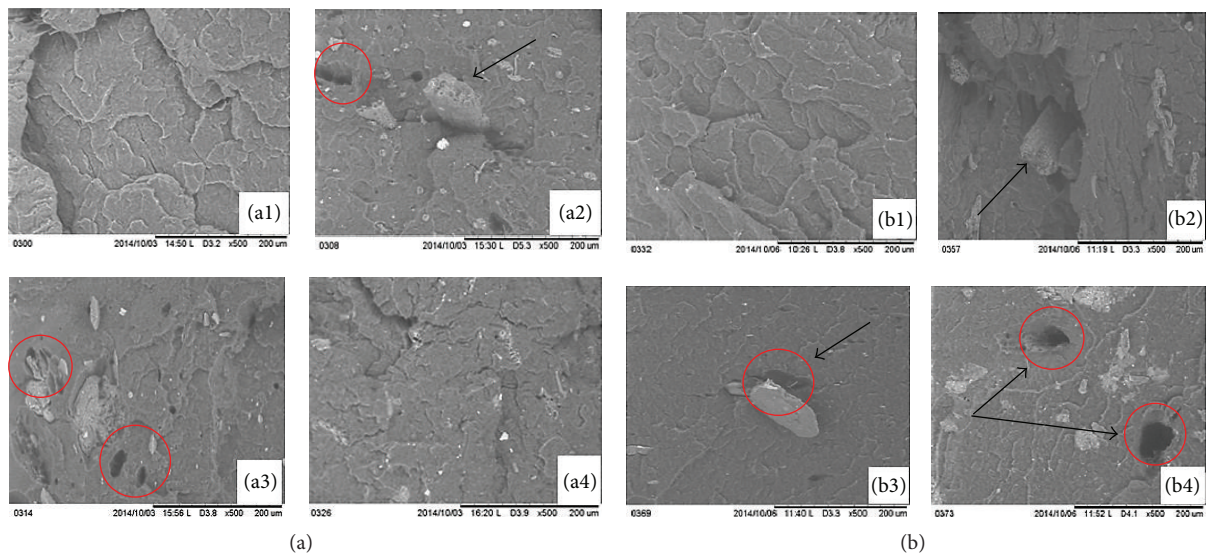


FIGURE 5: SEM micrographs of fractured surfaces (a) before aging and (b) after aging for composites: ((a1), (b1)) virgin PP, ((a2), (b2)) F20UT, ((a3), (b3)) F20AT, and ((a4), (b4)) F20AMAT.

which is generated by the diffusion of water molecules in the amorphous phase, may be responsible for such damage.

3.6. Scanning Electron Microscopy (SEM). The morphology and facies rupture were observed to evaluate changes induced by fiber incorporation in the polymeric matrix because the functional properties of the resulting material are directly related to the surface features of the composite and the interfacial adhesion between its components. The results are represented in Figures 5(a) and 5(b), which correspond to the fracture surface before and after hydrothermal aging, respectively. In particular, in Figure 5(a1), the facies of virgin PP before aging exhibits a very smooth relief. In contrast, in Figure 5(b1), the surface exhibits very few defects after 1000 h, likely because the surface of the virgin PP did not undergo degradation. As expected, the SEM micrographs

show that the addition of F20UT to the PP matrix before aging (Figure 5(a2)) resulted in a gap or void between the fiber elements and matrix. We can also notice the presence of aggregates in the F20UT composite. The formation of these aggregates affect negatively a dispersion of the alfa fiber in the matrix inducing the debonding which increased after aging (Figure 5(b2)) between these two components. The debonding load/matrix was often accompanied by shrinkage of the polymer around the load and can be reversed after the first instance. This phenomenon is attributed to hydrolysis of the polymer matrix by water [31]. The same result was observed for the formulations F20AT and F20AMAT (Figures 5(b3) and 5(b4)). Therefore, sample degradation was caused by debonding at the load/matrix interface. As a result, hollows and wide grooves that amounted to cracks were visible [32].

4. Conclusion

This study addresses the evolution of properties of untreated and treated alfa fiber-reinforced polypropylene composites during hydrothermal aging. Regardless of the type of treatment (acetylation by acetic anhydride or addition of the MAPP compatibilizing agent), the PP/alfa fiber composites showed a reduction in tensile moduli after aging. This decrease can be plausibly explained by the hydrophilic nature of the fiber that absorbs more moisture and causes swelling of the PP matrix. Rupture facies confirmed the debonding of alfa fiber elements, which in turn may participate in the decrease in mechanical properties of the composite. Concerning thermal properties, the incorporation of acetylation-treated and untreated alfa fibers before aging improved the thermal stability of the composites. In addition, the use of MAPP compatibilizer provided improved thermal stability compared with that observed with the acetylation-treated and untreated alfa fibers. After hydrothermal aging, the treated composites displayed a higher thermal stability, as evidenced by the increase in the onset temperature and the decrease of the maximum rate of degradation. This effect might be due to the stronger interactions between the fiber and matrix caused by the formation of covalent bonds at the interface in the presence of MAPP. The degrees of crystallinity of the treated and untreated samples decreased after hydrothermal aging due to the humidity; this change was corroborated by the DMA results.

Conflict of Interests

The authors declare that there is no conflict of interests regarding the publication of this paper.

Acknowledgments

The authors thank the University of Bejaia (Algeria) for its financial assistance with Noura Hamour's traveling expenses. The authors are also pleased to acknowledge François Gaudard and Pr. Vincent Barbin (URCA) for their help and the use of the SEM facilities.

References

- [1] A. Boukerrou, N. Hamour, H. Djidjelli, and D. Hammiche, "Effect of the different sizes of the alfa on the physical, morphological and mechanical properties of PVC/alfa composites," *Macromolecular Symposia*, vol. 321-322, no. 1, pp. 191-196, 2012.
- [2] D. Hammiche, A. Boukerrou, H. Djidjelli, M. Beztout, and S. Krim, "Synthesis of a new compatibilisant agent PVC-g-MA and its use in the PVC/alfa composites," *Journal of Applied Polymer Science*, vol. 124, no. 5, pp. 4352-4361, 2012.
- [3] B. Amar, K. Salem, D. Hocine, I. Chadia, and M. J. Juan, "Study and characterization of composites materials based on polypropylene loaded with olive husk flour," *Journal of Applied Polymer Science*, vol. 122, no. 2, pp. 1382-1394, 2011.
- [4] M. Tagdemir, H. Biltekin, and G. T. Caneba, "Preparation and characterization of LDPE and pp-wood fiber composites," *Journal of Applied Polymer Science*, vol. 112, no. 5, pp. 3095-3102, 2009.
- [5] A. Viksne, A. K. Bledzki, L. Rence, and R. Berzina, "Water uptake and mechanical characteristics of wood fiber-polypropylene composites," *Mechanics of Composite Materials*, vol. 42, no. 1, pp. 73-82, 2006.
- [6] H. Demir, U. Atikler, D. Balköse, and F. Tihminlioğlu, "The effect of fiber surface treatments on the tensile and water sorption properties of polypropylene-luffa fiber composites," *Composites A: Applied Science and Manufacturing*, vol. 37, no. 3, pp. 447-456, 2006.
- [7] M. N. Islam, M. R. Rahman, M. M. Haque, and M. M. Huque, "Physico-mechanical properties of chemically treated coir reinforced polypropylene composites," *Composites Part A: Applied Science and Manufacturing*, vol. 41, no. 2, pp. 192-198, 2010.
- [8] J. Beaugrand and F. Berzin, "Lignocellulosic fiber reinforced composites: influence of compounding conditions on defibrization and mechanical properties," *Journal of Applied Polymer Science*, vol. 128, no. 2, pp. 1227-1238, 2013.
- [9] S. Ochi, "Mechanical properties of kenaf fibers and kenaf/PLA composites," *Mechanics of Materials*, vol. 40, no. 4-5, pp. 446-452, 2008.
- [10] T. Huber, J. Müssig, O. Curnow, S. Pang, S. Bickerton, and M. P. Staiger, "A critical review of all-cellulose composites," *Journal of Materials Science*, vol. 47, no. 3, pp. 1171-1186, 2012.
- [11] E. Bodros, I. Pillin, N. Montrelay, and C. Baley, "Could biopolymers reinforced by randomly scattered flax fibre be used in structural applications?" *Composites Science and Technology*, vol. 67, no. 3-4, pp. 462-470, 2007.
- [12] N. P. J. Dissanayake, J. Summerscales, S. M. Grove, and M. M. Singh, "Life cycle impact assessment of flax fibre for the reinforcement of composites," *Journal of Biobased Materials and Bioenergy*, vol. 3, no. 3, pp. 245-248, 2009.
- [13] G. Cantero, A. Arbelaiz, F. Mugika, A. Valea, and I. Mondragon, "Mechanical behavior of wood/polypropylene composites: effects of fibre treatments and ageing processes," *Journal of Reinforced Plastics and Composites*, vol. 22, no. 1, pp. 37-50, 2003.
- [14] P. V. Joseph, G. Mathew, K. Joseph, G. Groeninckx, and S. Thomas, "Dynamic mechanical properties of short sisal fibre reinforced polypropylene composites," *Composites Part A: Applied Science and Manufacturing*, vol. 34, no. 3, pp. 275-290, 2003.
- [15] F. Ayadi and P. Dole, "Stoichiometric interpretation of thermoplastic starch water sorption and relation to mechanical behavior," *Carbohydrate Polymers*, vol. 84, no. 3, pp. 872-880, 2011.
- [16] A. K. Bledzki, M. Letman, A. Viksne, and L. Rence, "A comparison of compounding processes and wood type for wood fibre-PP composites," *Composites A: Applied Science and Manufacturing*, vol. 36, no. 6, pp. 789-797, 2005.
- [17] S. M. Luz, J. Del Tio, G. J. M. Rocha, A. R. Gonçalves, and A. P. Del'Arco Jr., "Cellulose and cellulignin from sugarcane bagasse reinforced polypropylene composites: effect of acetylation on mechanical and thermal properties," *Composites Part A*, vol. 39, no. 9, pp. 1362-1369, 2008.
- [18] D. Roy, S. Massey, A. Adnot, and A. Rjeb, "Action of water in the degradation of low-density polyethylene studied by X-ray photoelectron spectroscopy," *Express Polymer Letters*, vol. 1, no. 8, pp. 506-511, 2007.
- [19] N. Guermazi, K. Elleuch, and H. F. Ayedi, "The effect of time and aging temperature on structural and mechanical properties

- of pipeline coating," *Materials & Design*, vol. 30, no. 6, pp. 2006–2010, 2009.
- [20] S. M. B. Nachtigall, G. S. Cerveira, and S. M. L. Rosa, "New polymeric-coupling agent for polypropylene/wood-flour composites," *Polymer Testing*, vol. 26, no. 5, pp. 619–628, 2007.
- [21] E. Jakab, G. Várhegyi, and O. Faix, "Thermal decomposition of polypropylene in the presence of wood-derived materials," *Journal of Analytical and Applied Pyrolysis*, vol. 56, no. 2, pp. 273–285, 2000.
- [22] H. Yang, R. Yan, H. Chen, D. H. Lee, and C. Zheng, "Characteristics of hemicellulose, cellulose and lignin pyrolysis," *Fuel*, vol. 86, no. 12-13, pp. 1781–1788, 2007.
- [23] M. D. H. Beg and K. L. Pickering, "Reprocessing of wood fibre reinforced polypropylene composites. Part II: hygrothermal ageing and its effects," *Composites Part A*, vol. 39, no. 9, pp. 1565–1571, 2008.
- [24] H.-S. Kim, S. Kim, H.-J. Kim, and H.-S. Yang, "Thermal properties of bio-flour-filled polyolefin composites with different compatibilizing agent type and content," *Thermochimica Acta*, vol. 451, no. 1-2, pp. 181–188, 2006.
- [25] N. Olivares, P. Tiemblo, and J. M. Gómez-Elvira, "Physicochemical processes along the early stages of the thermal degradation of isotactic polypropylene I. Evolution of the γ relaxation under oxidative conditions," *Polymer Degradation and Stability*, vol. 65, no. 2, pp. 297–302, 1999.
- [26] N. Shiraishi, T. Matsunaga, T. Yokota, and Y. Hayashi, "Preparation of higher aliphatic acid esters of wood in an N₂O₄-DMF cellulose solvent medium," *Journal of Applied Polymer Science*, vol. 24, no. 12, pp. 2347–2359, 1979.
- [27] A. Espert, F. Vilaplana, and S. Karlsson, "Comparison of water absorption in natural cellulosic fibres from wood and one-year crops in polypropylene composites and its influence on their mechanical properties," *Composites A: Applied Science and Manufacturing*, vol. 35, no. 11, pp. 1267–1276, 2004.
- [28] D. Hammiche, A. Boukerrou, H. Djidjelli, Y.-M. Corre, Y. Grohens, and I. Pillin, "Hydrothermal ageing of alfa fiber reinforced polyvinylchloride composites," *Construction and Building Materials*, vol. 47, pp. 293–300, 2013.
- [29] Y. Chen, J. F. Davalos, I. Ray, and H. Y. Kim, "Accelerated aging tests for evaluations of durability performance of FRP reinforcing bars for concrete structures," *Composite Structures*, vol. 78, no. 1, pp. 101–111, 2007.
- [30] T.-T. Doan, H. Brodowsky, and E. Mäder, "Jute fibre/polypropylene composites II. Thermal, hydrothermal and dynamic mechanical behaviour," *Composites Science and Technology*, vol. 67, no. 13, pp. 2707–2714, 2007.
- [31] R. K. Rowe, S. Rimal, and H. Sangam, "Ageing of HDPE geomembrane exposed to air, water and leachate at different temperatures," *Geotextiles and Geomembranes*, vol. 27, no. 2, pp. 137–151, 2009.
- [32] H. N. Dhakal, Z. Y. Zhang, and M. O. W. Richardson, "Effect of water absorption on the mechanical properties of hemp fibre reinforced unsaturated polyester composites," *Composites Science and Technology*, vol. 67, no. 7-8, pp. 1674–1683, 2007.



Hindawi

Submit your manuscripts at
<http://www.hindawi.com>

